This is a preprint, the final version is subject to change, of the American Mineralogist (MSA)
Cite as Authors (Year) Title. American Mineralogist, in press.
(DOI will not work until issue is live.) DOI: http://dx.doi.org/10.2138/am-2017-6092

Revision 2

Crystal structure of richetite revisited: crystallographic evidence for the presence of pentavalent uranium

JAKUB PLÁŠIL[1*]

[1] Institute of Physics ASCR, v.v.i., Na Slovance 2, CZ–182 21, Praha 8, Czech Republic,

*email: plasil@fzu.cz

ABSTRACT:

Revision of crystal structure of the rare U-oxide mineral richetite provided crystallographic evidence for the presence of pentavalent U. The structure of richetite, space group *P*–1, *a* = 12.0919(2), *b* = 16.3364(4), *c* = 20.2881(4) Å, α = 68.800(2)°, β = 78.679(2)°, γ = 76.118(2)°, with *V* = 3600.65(14) Å^3 and *Z* = 1, was solved by charge-flipping algorithm and refined to an agreement index (*R*) of 5.6% for 9955 unique reflections collected using microfocus X-ray source. The refined structure, in line with the previous structure determination, contains U-O-OH sheets of the α-U_3O_8 type (protasite topology) and an interstitial complex comprising Pb^{2+}, Fe^{2+}, Mg^{2+} cations and molecular H_2O. However, the polyhedral geometry, the bond-valence sum incident at one U site within the sheet (U17) together with charge-balance requirements, indicate that U17 site is occupied by U^{5+}. The U17Φ_7 (Φ: O, OH) polyhedra is rather distorted, with two shorter U–O bond-lengths (~2.01 Å), four longer U–O bond-lengths (~2.2 Å) and one, very long U–O bond (2.9 Å). The color of richetite also supports the presence of U^{5+} in the structure The current results show that α-U_3O_8 type of sheet can incorporate U^{5+}. Richetite is the second mineral containing pentavalent uranium in Nature.

Keywords: Richetite, uranyl oxide hydroxy-hydrate, crystal structure, pentavalent uranium, weathering

Running title: Pentavalent U in richetite

INTRODUCTION

Uranyl-oxide hydroxy-hydrate minerals (further labelled as UOH) are important products of supergene weathering of primary U^{4+} minerals, predominantly uraninite. They form in the initial alteration stages and are common constituents of the oxidized parts of uranium deposits, and usually replace uraninite *in-situ*, forming massive aggregates called "*gummites*" (Finch and Ewing 1992; Finch and Murakami 1999; Krivovichev and Plášil 2013; Plášil 2014). Weathering of uraninite, also called hydration-oxidation weathering, is of further relevance because of the analogy between the alteration of uraninite and UO_{2+x} in spent nuclear fuel (Janeczek et al. 1996). The crystallography and crystal chemistry of this mineral group has attracted a lot of attention and this group is nowadays extensive (see e.g., Plášil et al. 2016). These minerals and the synthetic UOH phases have been studied intensively by X-ray diffraction and only a few of their structures are unknown.

Richetite is a rare UOH mineral, occurring at few localities in the world. It was originally described by Vaes (1947) from Shinkolobwe mine, Haut-Katanga province, Democratic Republic of Congo, Africa, and later studied by Piret and Deliens (1984). Richetite has a large triclinic unit-cell (Burns 1998), which is in line with results of Piret and Deliens (1984). However, the structure has several issues prompting reexamination of the structure.

REDETERMINATION OF THE CRYSTAL STRUCTURE

Single-crystal X-ray diffraction

The crystal used in this study was obtained from a sample provided by Jean-Claude Leydet (Brest, France) and originates from the type locality, Shinkolobwe mine (Haut-Katanga province, DRC, Africa).

A tabular greyish brown fragment of richetite was selected under an optical microscope and used for X-ray study. Data were collected using a Rigaku (Oxford diffraction) SuperNova diffractometer, using Mo$K\alpha$ radiation (λ = 0.71073 Å) from a micro-focus X-ray tube collimated and monochromatized by mirror optics and detected by an Atlas S2 CCD detector. From 39599 collected reflections, 13469 were independent and 9955 were unique observed with the criterion $I_{obs} > 3\sigma(I)$. Integration of the diffraction data, including corrections for background, polarization and Lorentz effects, was done using the CrysAlis RED program. The absorption correction combining empirical scaling and spherical-absorption correction was done with CrysAlis program; SCALE3 Abspack algorithm.

The structure of richetite was solved by the charge-flipping algorithm using the Shelxt program (Sheldrick 2015). The structure model was refined by full-matrix least-squares in the Jana2006 program (Petříček et al. 2014) based on F^2. The reflection conditions were consistent with the space-group P–1, which was further confirmed by the successful refinement. The possibility for twinning by reticular merohedry was tested by Jana2006 (Petříček et al. 2016) (transformation matrix 1 -2 -1/1 0 0/0 -1 1), however it was negative. The crystal used for the experiment was found to be a split crystal; the contribution of the second fragment to the dataset was corrected by detecting fully separated, fully overlapped and partially separated reflections in Jana2006 (Petříček et al. 2016). The structure solution provided nearly complete structure sheets and missing atoms (mostly O atoms) were located from the difference-Fourier maps. Anisotropic displacement parameters were used for U, Pb and Fe atoms. Unconstrained and unrestrained refinement converged smoothly to final R = 0.056 for 9955 unique observed reflections (Table 1). Final atom coordinates and displacement parameters are listed in Tables 2 and 1S (Supplementary file), selected interatomic distances are in Tables 3 and 4, and the bond-valence sums (calculated by the procedure of Brown, 1981, 2002) are listed in Table 2. The original crystallographic

information file (cif) is provided as Supplementary material and can be downloaded from XXXX.

DESCRIPTION OF THE CRYSTAL STRUCTURE

The structure of richetite contains 18 unique U sites, 8 unique Pb sites, 1 mixed Fe/Mg site, and 85 O sites (of which 18 correspond to H_2O groups) (Fig. 1). The U sites are coordinated by seven ligands (O or OH^-) in two classes of distances: ~1.8 Å and 2.1 to ~2.8 Å. as it is characteristic for the UO_2^{2+} ion (Evans 1963; Burns et al. 1997a; Lussier et al. 2016). The structure contains 8 Pb sites; none of them is fully occupied, site-scattering refinement showed occupancies ranging from 0.14 to 0.95. The coordination polyhedra around Pb atoms are irregular; ligands are represented by O_{Ur} atoms and H_2O groups, with Pb–Φ bond-lengths ranging from 2.4 to 3.1 Å (Table 5). Richetite structure contains also one symmetrically unique octahedrally coordinated site, occupied by divalent cations Fe^{2+} and Mg^{2+}, with $<M^{2+}$–Φ> bond-length of 2.07 Å. The M^{2+} octahedron is quite regular and is formed by two O_{Ur} atoms (of the U2) and four H_2O groups. Site-scattering refinement gave M^{2+} = 0.62 Fe^{2+} + 0.38 Mg^{2+}.

The U17 site

Several U sites in the structure of richetite exhibit rather irregular coordination. In case of U17 (Fig. 2; Table 4) O62 and O72 atoms (OH groups), which usually should be O_{Ur} atoms with U–O bond-lengths of 1.8 Å, have U–O distances of 2.006(19) and 2.01(2) Å. Moreover, O62–U17–O72 bond-angle is 171.82°, different from the usually linear UO_2^{2+} ion. Bond-valence analysis (Table 2) indicates that the U17 site is occupied by pentavalent U.

The sheets of polyhedra

105 The sheet of polyhedra found in richetite has the protasite uranyl–anion topology, i.e.
106 the α-U_3O_8 sheet (Fig. 3) (Burns 1998, 2005; Lussier et al., 2016). All pentagons are occupied
107 by U atoms, the U17 site by U^{5+}, and the rest by U^{6+}. Based upon distribution of $(OH)^-$ within
108 the equatorial ligands (excluding two OH groups associated with U17), we can distinguish
109 several structures of protasite topology. In richetite (Burns 1998), we have the AABAAB…
110 sequence, where considering type-A triangles (which have (OH) groups at all corners), and
111 type-B triangles (which contain only O^{2-} anions), richetite has twice as many A triangles as B
112 triangles. The O:OH ratio in richetite is 3:2, however, there are also two OH groups linked to
113 U17 (in case of other U sites in richetite, they are O_{Ur} atoms), linking U17 to Pb1 through
114 O62, and to Pb4 and Pb7 through O72. In case of protasite (Pagoaga et al. 1987), all (OH)
115 groups are located at the corners of triangles of the topology, such that all triangles in the
116 sheet contain two (OH) groups. The sheets in the structures of becquerelite (Burns and Li
117 2002) and billietite (Finch et al. 2006) (considering there the α-U_3O_8 sheet only) have the
118 composition $[(UO_2)_6O_4(OH)_6]^{2-}$ with O:OH = 2:3. In the becquerelite and billietite sheet
119 anion-topologies, all (OH) groups are located at the corners of triangles, and all triangles
120 contain three (OH) groups.
121
122 *The interlayer complex*
123 As indicated by Burns (1998), the structure of richetite contains two different
124 interlayer complexes containing Pb^{2+}, M^{2+} and H_2O groups. Adjacent sheets of protasite
125 topology are linked through an extensive network of Pb–O, M^{2+}–O and O–H…O bonds. The
126 interstitial complex comprising M^{2+} octahedra occurs at **b** = 0, **c** = 0 and is built from two
127 tetramers (Pb2, Pb4, Pb7 and Pb8) linked by M^{2+} octahedra (Fig. 4). Four of the ligands
128 coordinated to M^{2+} site are H_2O groups, and two are O_{Ur} atoms. There is an additional O site

(O84) that is occupied by an H_2O group that links to the structure through H-bonds only. The coordination environment of the corresponding Pb sites is shown in Fig. 4.

The interlayer complex that does not contain the M^{2+} site occurs at **b**~0.5, **c**~0.5. It contains a dimer of $Pb1\Phi_8$ and $Pb3\Phi_9$ (Φ = O, OH, H_2O) polyhedra and a tetramer of $Pb5\Phi_8$ and $Pb6\Phi_8$ (Φ = O, H_2O) polyhedra (Fig. 5). Between these clusters of polyhedra there are three independent O sites that belong to H_2O groups that are not coordinated directly to any metal cation site.

The structural formula

The structural formula of the studied richetite crystal is therefore $M^{2+}_{0.50}Pb_{4.86}[U^{5+}(U^{6+}O_2)_{17}O_{18}(OH)_{14}](H_2O)_{\sim 19.5}$, $Z = 2$. This formula is in line with the color of richetite (Fig. 6). Most UOH minerals are orange or yellow, whereas those minerals containing U^{5+}, wyartite (Burns and Finch 1999) and dehydrated wyartite (Hawthorne et al. 2006) are similar in color to richetite.

α-U_3O_8 topology and the presence of U^{5+}

Incorporation of U^{5+} into α-U_3O_8 type sheets has not been considered; all minerals with U^{5+} or U^{4+} present adopt β-U_3O_8 sheets (Burns and Finch 1999; Burns et al. 1997b; Hawthorne et al. 2006). For shinkolobweite, $Pb_{1.25}[U^{5+}(H_2O)_2(UO_2)_5O_8(OH)_2](H_2O)_5$ (Olds et al. 2017), there are sheets resembling β-U_3O_8 topology. Geometrically, the U17 site in richetite is consonant with the idealized α-U_3O_8 topology and bond-valence analysis clearly indicates incorporation of U^{5+}. Thus, incorporation of U^{5+} into α-U_3O_8 topology is possible.

THE ROLE OF RICHETITE IN URANINITE ALTERATION

153 UOH minerals are important products of oxidation-hydration weathering of uraninite,
154 or UO_2 in spent nuclear fuel (Finch and Ewing 1992; Janeczek et al. 1996; Wronkiewicz et al.
155 1992, 1996; Krivovichev and Plášil 2013; Plášil 2014). Based on field as well as laboratory
156 observations (for references, see above cited papers), a weathering sequence for UOH has
157 been established (after Finch and Ewing 1992; Fig. 7). At very early stages of uraninite
158 alteration under oxidizing conditions, result in minerals with a high-proportion of molecular
159 H_2O and low content of metal cations such as schoepite, $[(UO_2)_8O_2(OH)_{12}](H_2O)_{12}$ (Finch et
160 al. 1996, 1998). With increasing time UOH structures will incorporate metal cations released
161 from the gradually weathering uraninite (such as radiogenic Pb, and others) or from host-
162 rocks (Na, K, Ca etc.). The position of richetite in the alteration sequence is determined by the
163 molar proportion of H_2O and *Me* close to fourmarierite, masuyite and protasite. Also the
164 value of charge deficiency per anion (CDA; defined by Schindler and Hawthorne 2008),
165 ~0.21 *v.u.*, is close to that of fourmarierite (0.19 *v.u.*) and masuyite (0.22 *v.u.*). It has been
166 shown that the CDA value correlates closely with increase of *Me* and decrease of H_2O in the
167 structures, therefore higher CDA corresponds to older products during the weathering
168 sequence. There are two or three other UOH minerals that contain reduced forms of U. They
169 are ianthinite (with U^{4+}), wyartite and dehydrated wyartite (with U^{5+} in addition to U^{6+}). The
170 presence of the reduced form of an easily oxidized species indicates high gradients of redox
171 conditions within the systems where these phases form. All of these phases form during initial
172 stages of uraninite weathering. Ianthinite is related to the schoepite family of minerals (Fig.
173 7); there is a solid-state spontaneous phase transition from ianthinite to schoepite. The
174 position of wyartite is not clear; the usual mineral association comprises uranophane,
175 schoepite and fourmarierite. Samples of ianthinite, besides those from Shinkolobwe, also
176 come from the well-known uranium deposit Menzenschwand (Krunkelbachtal, Baden-
177 Württemberg, Germany), where ianthinite is usually associated with pyrite and often fills

vugs in altered uraninite-pyrite aggregates in a quartz matrix. Richetite forms during later stages of uraninite weathering. The presence of Fe^{2+} in richetite also indicates special geochemical conditions. It seems likely that most of sulfides (as a source of Fe) had undergone complete dissolution prior to the formation of richetite. It is clear that partial reduction of U^{6+} to U^{5+} is most probably connected to the Fe^{2+}/Fe^{3+} pair, which is also the most frequent redox agent in Nature. To assess the role of Fe in the formation of richetite, more detailed textural work is needed. To conclude, minerals where U is present in a reduced valence state, such as in ianthinite, wyartite and richetite, may play an important role during the alteration of uraninite or SNF under less-oxidizing conditions, or at places with reduced fO_2 or where the redox conditions are characterized by high gradients, as in roll-front, environments with extremely low pH etc. Such phases also might play role during long-term storage of SNF in geological repositories under reducing conditions (Ewing 2015; Ewing et al. 2016).

ACKNOWLEDGEMENTS

Jean-Claude Leydet (Brest, France) is thanked for providing me a sample for single-crystal study. My thanks go to Jiří Čejka (Roudnice nad Labem, Czech Republic) for his encouragement for the study and critical reading of the manuscript and to Stephan Wolfsried (Waiblingen, Germany) for beautiful microphotography or richetite crystals. The manuscript benefited from the comprehensive thorough reviews of Sergey Krivovichev and an anonymous referee. The editorial handling of Peter Burns is highly acknowledged. This research was financially supported the project No. LO1603 under the Ministry of Education, Youth and Sports National sustainability program I of Czech Republic.

REFERENCES CITED

Bénard, P., Louër, D., Dacheux, N., Brandel, V. and Genet, M. (1994) $U(UO_2)(PO_4)_2$, a new mixed-valence uranium orthophosphate: ab initio structure determination from powder diffraction data and optical and X-ray photoelectron spectra. Chemistry of Materials, 6, 1049–1058.

Brown, I.D. (1981) The bond-valence method: an empirical approach to chemical structure and bonding. In Structure and Bonding in Crystals II (M. O'Keeffe & A. Navrotsky, eds.). Academic Press, New York, N.Y., 1–30.

Brown, I.D. (2002) The Chemical Bond in Inorganic Chemistry: The Bond Valence Model. Oxford University Press, UK.

Brown, I.D. (2009) Recent Developments in the Methods and Applications of the Bond Valence Model. Physical Reviews, 109, 6858–6919.

Brown, I.D. and Altermatt, D. (1985) Bond-valence parameters obtained from a systematic analysis of the inorganic crystal structure database. Acta Crystallographica, B41, 244−247, with updated parameters from http://www.ccp14.ac.uk/ccp/web-mirrors/i_d_brown/.

Burns, P.C. (1998) The structure of richetite, a rare lead uranyl oxide hydrate. Canadian Mineralogist, 36, 187–199.

Burns, P.C. (1999) A new complex sheet of uranyl polyhedra in the structure of wölsendorfite. American Mineralogist, 84, 1661–1673.

Burns, P.C. (2005) U6+ minerals and inorganic compounds: insights into an expanded structural hierarchy of crystal structures. Canadian Mineralogist, 43, 1839–1894.

Burns, P.C. and Finch, R.J. (1999) Wyartite: crystallographic evidence for the first pentavalent-uranium mineral. American Mineralogist, 84, 1456–1460.

Burns, P.C. and Li, Y. (2002) The structures of becquerelite and Srexchanged becquerelite. American Mineralogist, 87, 550–557.

Burns, P.C., Ewing, R.C. and Hawthorne, F.C. (1997a) The crystal chemistry of hexavalent uranium: polyhedron geometries, bond-valence parameters, and polymerization of polyhedra. Canadian Mineralogist, 35, 1551–1570.

Burns, P.C., Finch, R.J., Hawthorne, F.C., Miller, M.L. and Ewing, R.C. (1997b) The crystal structure of ianthinite, $[U^{4+}{}_2(UO_2)_4O_6(OH)_4(H_2O)_4](H_2O)_5$: a possible phase for Pu^{4+} incorporation during the oxidation of spent nuclear fuel. Journal of Nuclear Materials, 249, 199–206.

Busch, J. and Gruehn, R. (1994) Chemischer Transport und Struktur von UNb_2O_7–einem neien MM'_2O_7-Typ. Zeitschrift für Anorganische und Allgemeine Chemie, 620, 1066–1072.

Cordfunke, E.H.P., Van Vlaanderen, P.V., Goubitz, K. and Loopstra, B.O. (1985): Pentauranium(V) chloride dodecaoxide $U_5O_{12}Cl$. Journal of Solid State Chemistry, 56, 166–170.

Deliens, M. and Piret, P. (1996) Les Masuyites de Shinkolobwe (Shaba, Zaïre) constituent un groupe formé de deux variétés distinctes par leur composition chimique et leurs propriétés radiocristallographiques. Bulletin - Institut Royal des sciences naturelles de Belgique. Sciences de la Terre, 66, 187–192.

Dickens, P.G. and Stuttard, G.P. (1992) Structure of uranium antimony oxide ($USbO_5$) powder neutron diffraction study. Journal of Materials Chemistry, 2, 691–694.

Dickens, P.G., Stuttard, G.P, Ball, R.G.J., Powell, A.V., Hull, S. and Patat, S. (1992) Powder neutron diffraction study of the mixed uranium vanadium oxides $Cs_2(UO_2)_2(V_2O_8)$ and UVO_5. Journal of Materials Chemistry, 2, 161–166.

Evans, H.T., Jr. (1963) Uranyl ion coordination. Science, 141, 154–157.

Ewing, R.C. (2015) Long-term storage of spent nuclear fuel. Nature Materials, 14, 252–257.

Ewing, R.C., Whittlestone, L.A. and Yardley, B.W.D. (2016) Geological Disposal of Nuclear Waste: a Primer. Elements, 12, 233–237.

Finch, R.J. and Ewing, R.C. (1992) The corrosion of uraninite under oxidizing conditions. Journal of Nuclear Materials, 190, 133–156.

Finch, R.J. and Murakami, T. (1999) Systematics and paragenesis of uranium minerals. In: Burns PC, Ewing RC (eds) Uranium: Mineralogy, Geochemistry and the Environment. Mineralogical Society of America and Geochemical Society. Reviews in Mineralogy and Geochemistry, 38, 91–179.

Finch, R.J., Cooper, M.A., Hawthorne, F.C. and Ewing, R.C. (1996) The crystal structure of schoepite, $[(UO_2)_8O_2(OH)_{12}](H_2O)_{12}$. Canadian Mineralogist, 34, 1071–1088.

Finch, R.J., Hawthorne, F.C. and Ewing, R.C. (1998) Structural relations among schoepite, metaschoepite and "dehydrated schoepite". Canadian Mineralogist, 36, 831–845.

Finch, R.J., Burns, P.C., Hawthorne, F.C. and Ewing, R.C. (2006) Refinement of the crystal structure of billietite $Ba[(UO_2)_6O_4(OH)_6](H_2O)_8$. Canadian Mineralogist, 44, 1197–1205.

Hawthorne, F.C., Finch, R.J. and Ewing, R.C. (2006) The crystal structure of dehydrated wyartite, $Ca(CO_3)(U^{5+}(U^{6+}O_2)_2O_4(OH))(H_2O)_3$. Canadian Mineralogist, 44, 1379–1385.

Janeczek, J., Ewing, R.C., Oversby, V.M. and Werme, L.O. (1996) Uraninite and UO_2 in spent nuclear fuel: a comparison. Journal of Nuclear Materials, 238, 121–130.

Krivovichev, S.V. (2013) Structural complexity of minerals: information storage and processing in the mineral world. Mineralogical Magazine, 77, 275–326.

Krivovichev, S.V. and Brown, I.D. (2001) Are the compressive effects of encapsulation an artifact of the bond valence parameters? Zeitschrift für Kristallographie, 216, 245–247.

Krivovichev, S.V. and Plášil, J. (2013) Mineralogy and crystallography of uranium. in "Uranium, from cradle to grave", P.C. Burns and G.E. Sigmon, eds. MAC Short Course, 43, pp. 15–119, Winnipeg MB, May 2013.

Li, Y. and Burns, P.C. (2000a) Investigations of crystal-chemical variability in lead uranyl oxide hydrates. I. Curite. Canadian Mineralogist, 38, 727–735.

Li, Y. and Burns, P.C. (2000b) Investigations of crystal-chemical variability in lead uranyl oxide hydrates. II. Fourmarierite. Canadian Mineralogist, 38, 737–749.

Lussier, A.J., Lopez, R.A.K. and Burns, P.C. (2016) A Revised and Expanded Structure Hierarchy of Natural and Synthetic Hexavalent Uranium Compounds. Canadian Mineralogist, 54, 177–283.

Olds, T.A., Lussier A.J., Oliver, A.G., Petříček, V., Plášil, J., Kampf, A.R., Burns, P.C., Dembowski, M., Carlson, S.M. and Steele, I.M. (2017) Shinkolobweite, IMA 20XX-XXX. CNMNC Newsletter No. XX, XXX 2017, page XXX. Mineralogical Magazine, XX, XXX–XXX.

Pagoaga, M.K., Appleman, D.E. and Stewart, J.M. (1987) Crystal structures and crystal chemistry of the uranyl oxide hydrates becquerelite, billietite, and protasite. American Mineralogist, 72, 1230–1238.

Petříček, V., Dušek M. and Palatinus, L. (2014) Crystallographic Computing System JANA2006: General features. Zeitschrift für Kristallographie, 229, 345–352.

Petříček, V., Dušek, M. and Plášil, J. (2016) Crystallographic computing system Jana2006: solution and refinement of twinned structures. Zeitschrift für Kristallographie, 231, 583–599.

Piret, P. and Deliens, M. (1984) Nouvelles données sur la richetite $PbO.4UO_3.4H_2O$. Bulletin de Minéralogie, 107, 581–585.

Plášil, J. (2014) Oxidation–hydration weathering of uraninite: the current state-of-knowledge. Journal of Geosciences, 59, 99–114.

Plášil, J., Škoda, R., Čejka, J., Bourgoin, V. and Boulliard, J.-C. (2016) Crystal structure of the uranyl-oxide mineral rameauite. European Journal of Mineralogy, 28, 959–967.

Schindler, M. and Hawthorne, F.C. (2008) The stereochemistry and chemical composition of interstitial complexes in uranyl-oxysalt minerals. Canadian Mineralogist, 46, 467–501.

Serezhkin, Kovba, L.M., and Trunov, V.K. (1973) Crystal structure of U_2MoO_8. Kristallografiya, 18, 514–517. (in Russian)

Sheldrick, G.M. (2015) SHELXT - Integrated space-group and crystal-structure determination. Acta Crystallographica, A71, 3–8.

Siidra, O., Zenko, D.S. and Krivovichev, S.V. (2014) Structural complexity of lead silicates: Crystal structure of $Pb_{21}[Si_7O_{22}]_2[Si_4O_{13}]$ and its comparison to hyttsjoite. American Mineralogist, 99, 817–823.

Vaes, J.F. (1947) Six nouveaux minéraux d'urane provenant de Shinkolobwe (Katanga). Annal. Soc. Géol. Belg., 70, 212–225.

Wronkiewicz, D.J., Bates, J.K., Gerding, T.J. and Veleckis, E. (1992) Uranium release and secondary phase formation during unsaturated testing of UO_2 at 90°C. Journal of Nuclear Materials, 190, 107–127.

Wronkiewicz, D.J., Bates, J.K., Wolf, S.F. and Bick, E.C. (1996) Ten year results from unsaturated drip tests with UO_2 at 90°C: implications for the corrosion of spent nuclear fuel. Journal of Nuclear Materials, 238, 78–95.

Caption to Figures

FIGURE 1. Crystal structure of richetite viewed down **a**. Uranyl polyhedra are drawn in yellow color, except of U^{5+}17 polyhedra (red); M^{2+} octahedra are green, Pb atom dark grey and O atoms are displayed as red balls. Unit-cell edges are outlined in solid black line.

FIGURE 2. Coordination environment around U17 site, occupied by U^{5+}, with displayed bond-lengths and O–U–O bonding-angle.

FIGURE 3. Sheet of uranyl polyhedra of the α-U_3O_8 type (or protasite topology) found in the structure of richetite. In red is displayed U17 polyhedron, occupied by U^{5+}; the distribution of OH groups within the sheet is shown by blue balls.

FIGURE 4. Interstitial constituents at **b**~0, **c**~0 (extended to for about four unit-cell content). The M^{2+} (mixed Fe1/Mg1 site) octahedra are shown in green color, Pb^{2+}-sites are dark grey, O atoms are represented by red balls. H_2O groups are labelled (W).

FIGURE 5. Interstitial constituents at **b**~0.5, **c**~0.5 (extended to for about four unit-cell content). Pb^{2+}-sites are dark grey, O atoms are represented by red balls. H_2O groups are labelled (W).

FIGURE 6. Richetite crystals (olive brown) among masuyite (orange). Shinkolobwe mine (type locality), Haute-Katanga province, DRC, Africa. FOV 2 mm, photo S. Wolfsried.

FIGURE 7. Composition of uranyl-oxide hydroxy-hydrate minerals as a function of proportion of molecular H_2O and a content of metal cations (Me).

This is a preprint, the final version is subject to change, of the American Mineralogist (MSA)
Cite as Authors (Year) Title. American Mineralogist, in press.
(DOI will not work until issue is live.) DOI: http://dx.doi.org/10.2138/am-2017-6092

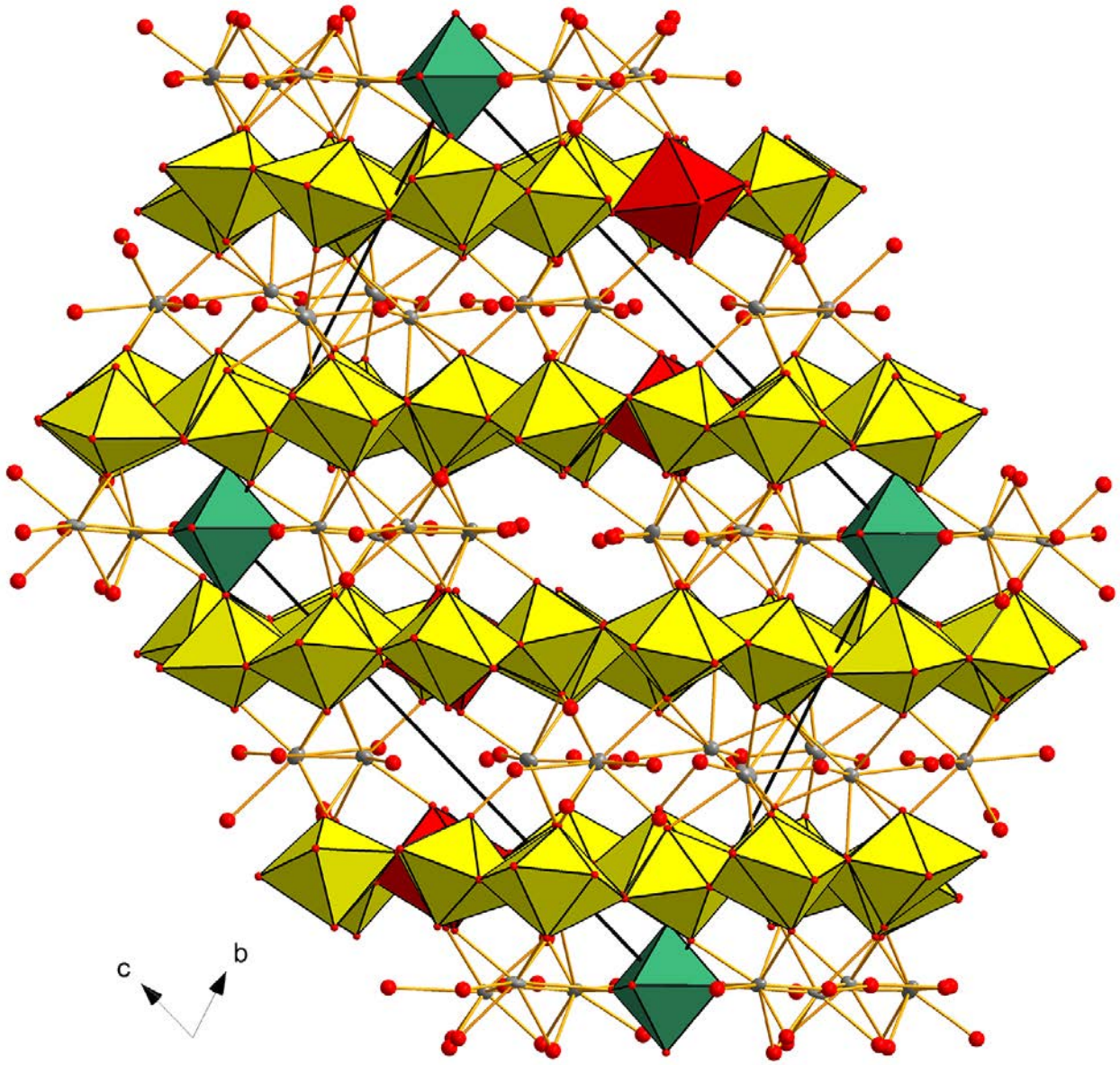

This is a preprint, the final version is subject to change, of the American Mineralogist (MSA)
Cite as Authors (Year) Title. American Mineralogist, in press.
(DOI will not work until issue is live.) DOI: http://dx.doi.org/10.2138/am-2017-6092

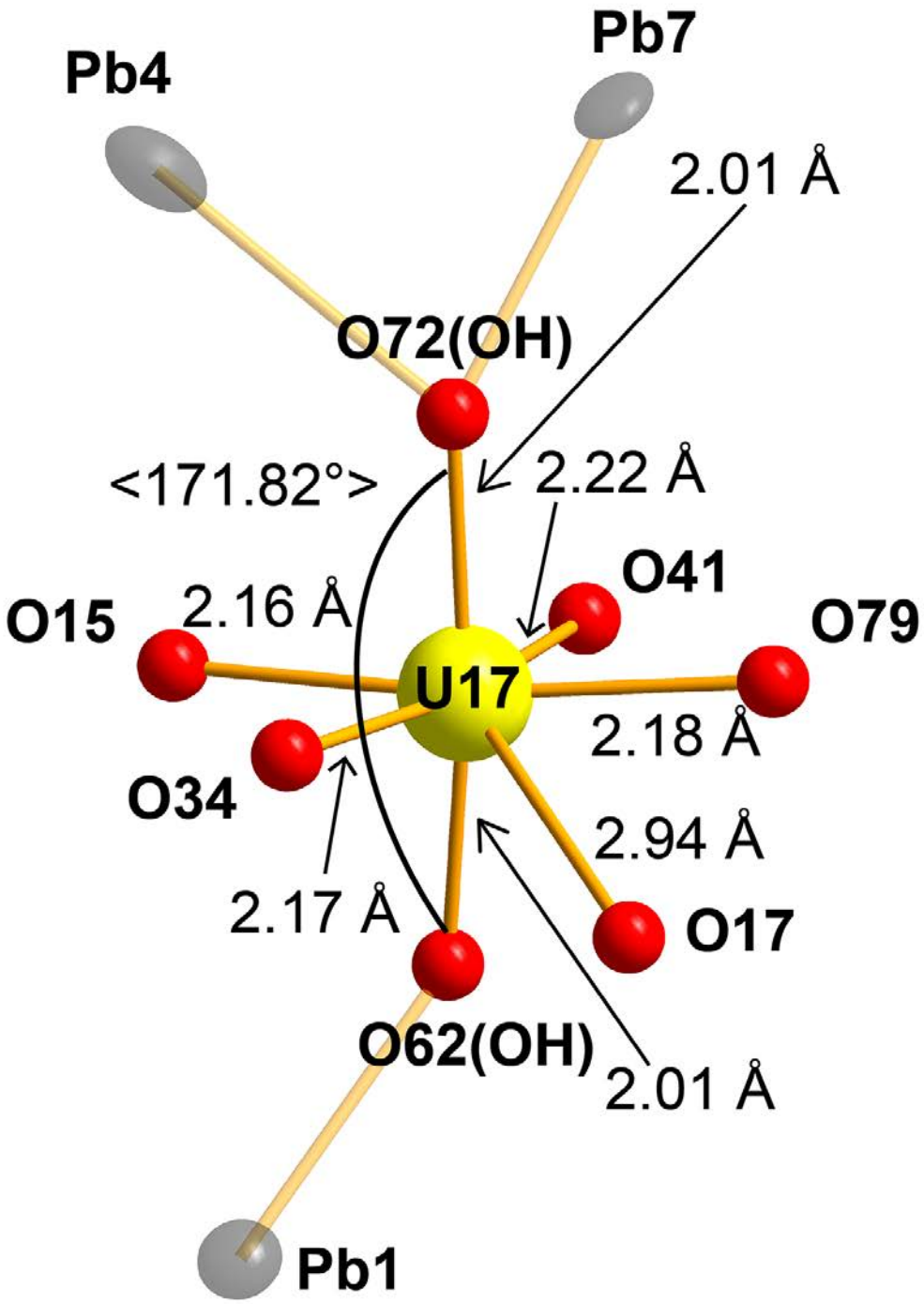

This is a preprint, the final version is subject to change, of the American Mineralogist (MSA)
Cite as Authors (Year) Title. American Mineralogist, in press.
(DOI will not work until issue is live.) DOI: http://dx.doi.org/10.2138/am-2017-6092

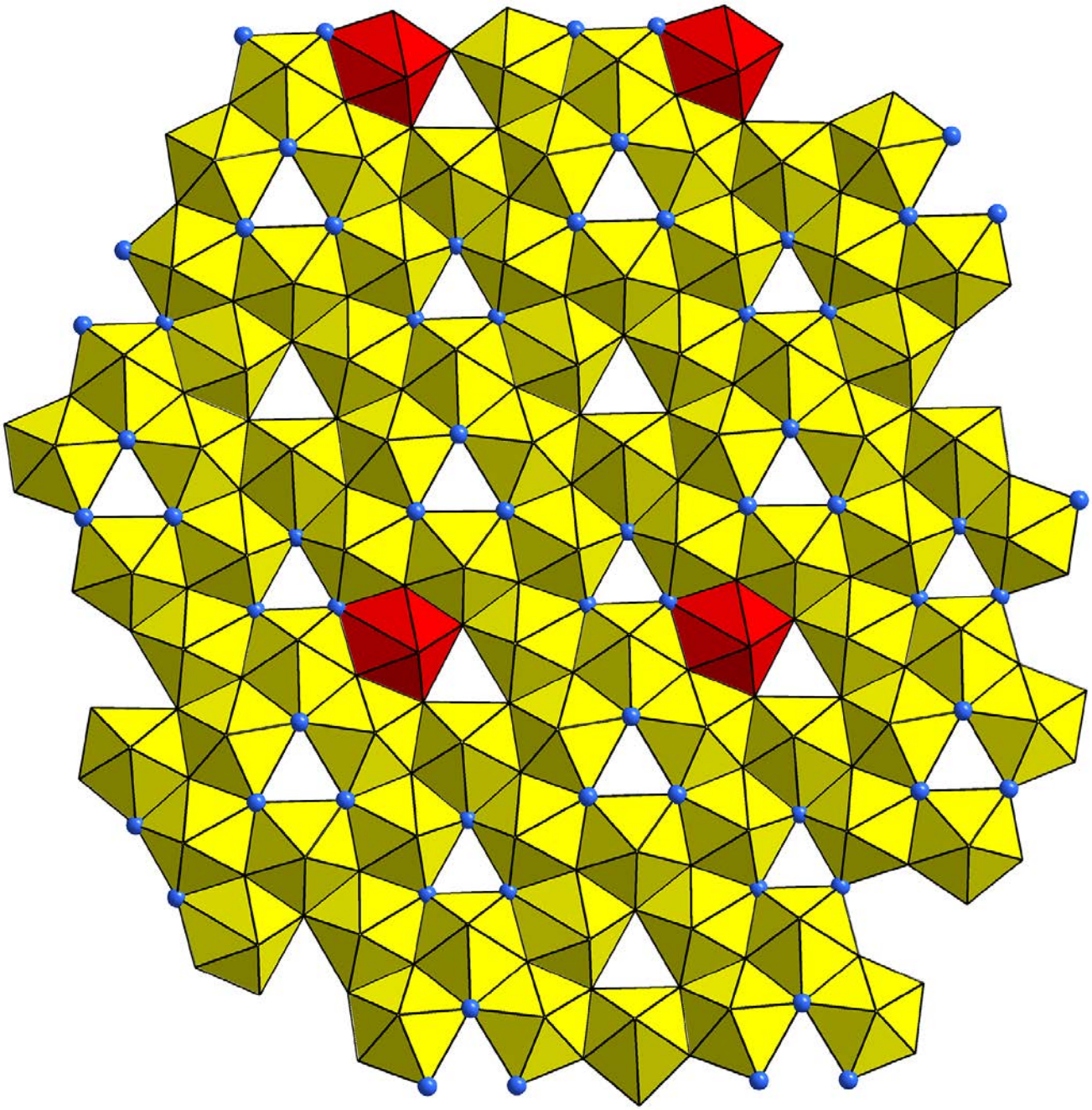

This is a preprint, the final version is subject to change, of the American Mineralogist (MSA)
Cite as Authors (Year) Title. American Mineralogist, in press.
(DOI will not work until issue is live.) DOI: http://dx.doi.org/10.2138/am-2017-6092

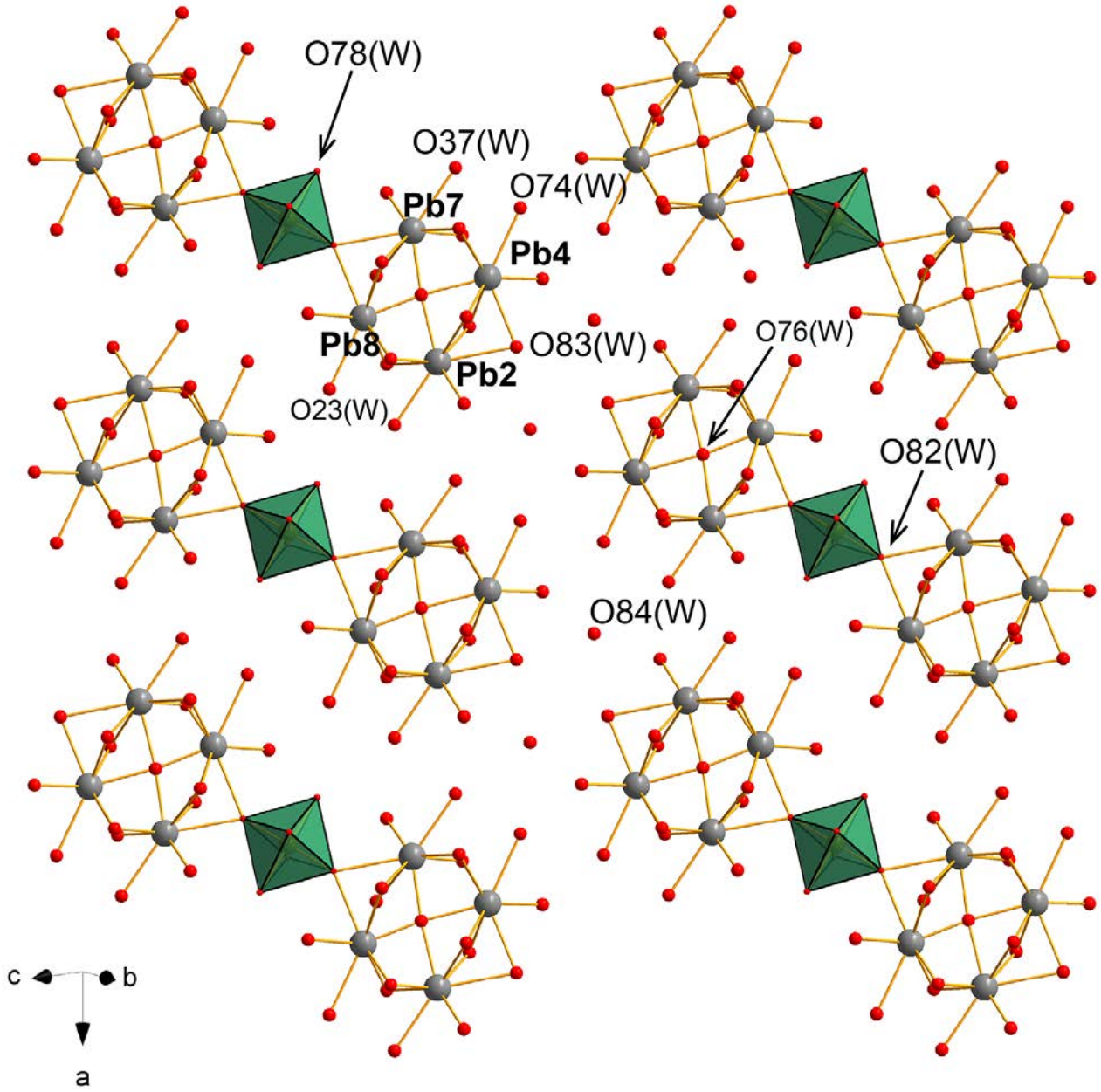

This is a preprint, the final version is subject to change, of the American Mineralogist (MSA)
Cite as Authors (Year) Title. American Mineralogist, in press.
(DOI will not work until issue is live.) DOI: http://dx.doi.org/10.2138/am-2017-6092

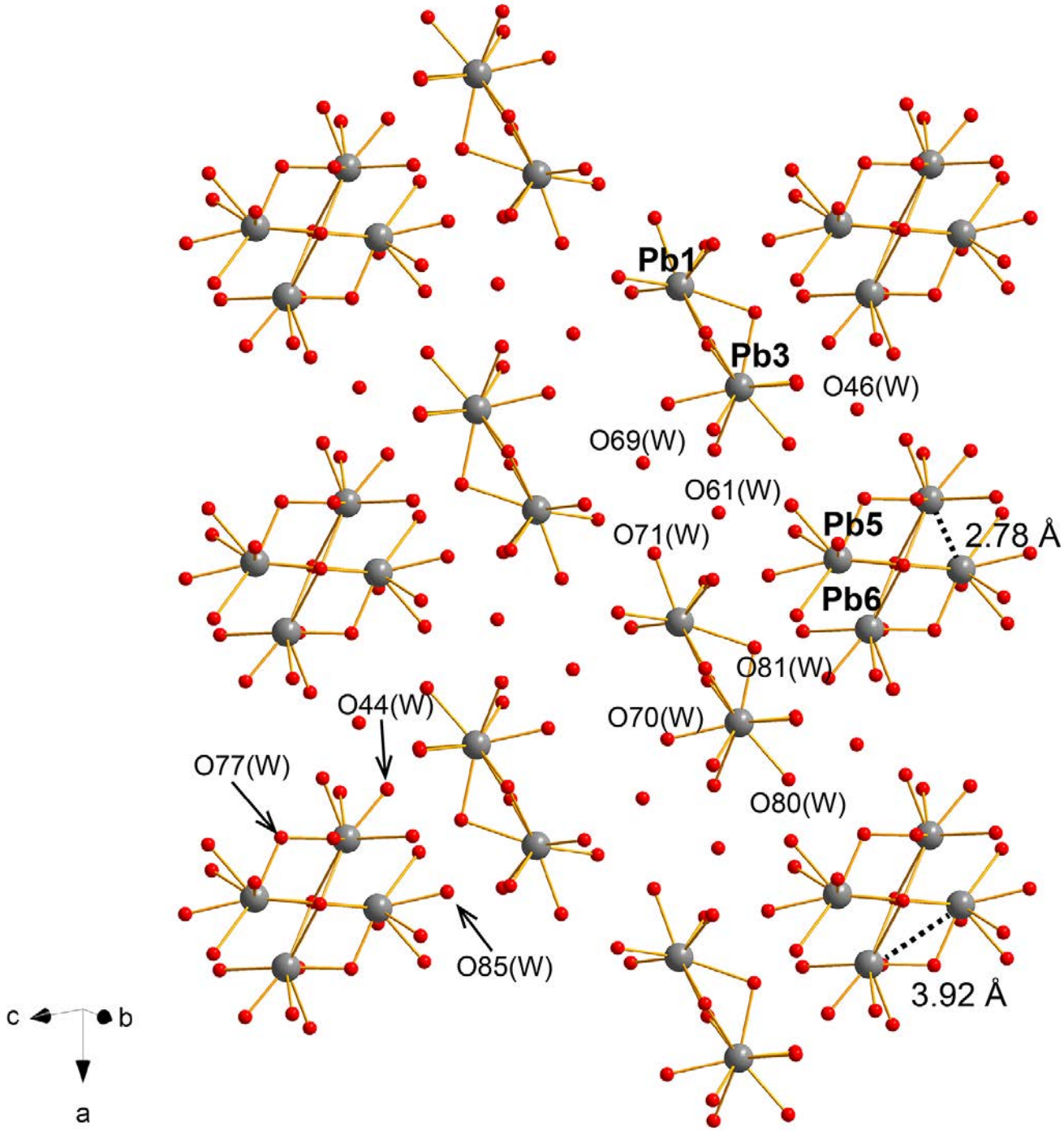

This is a preprint, the final version is subject to change, of the American Mineralogist (MSA)
Cite as Authors (Year) Title. American Mineralogist, in press.
(DOI will not work until issue is live.) DOI: http://dx.doi.org/10.2138/am-2017-6092

This is a preprint, the final version is subject to change, of the American Mineralogist (MSA)
Cite as Authors (Year) Title. American Mineralogist, in press.
(DOI will not work until issue is live.) DOI: http://dx.doi.org/10.2138/am-2017-6092

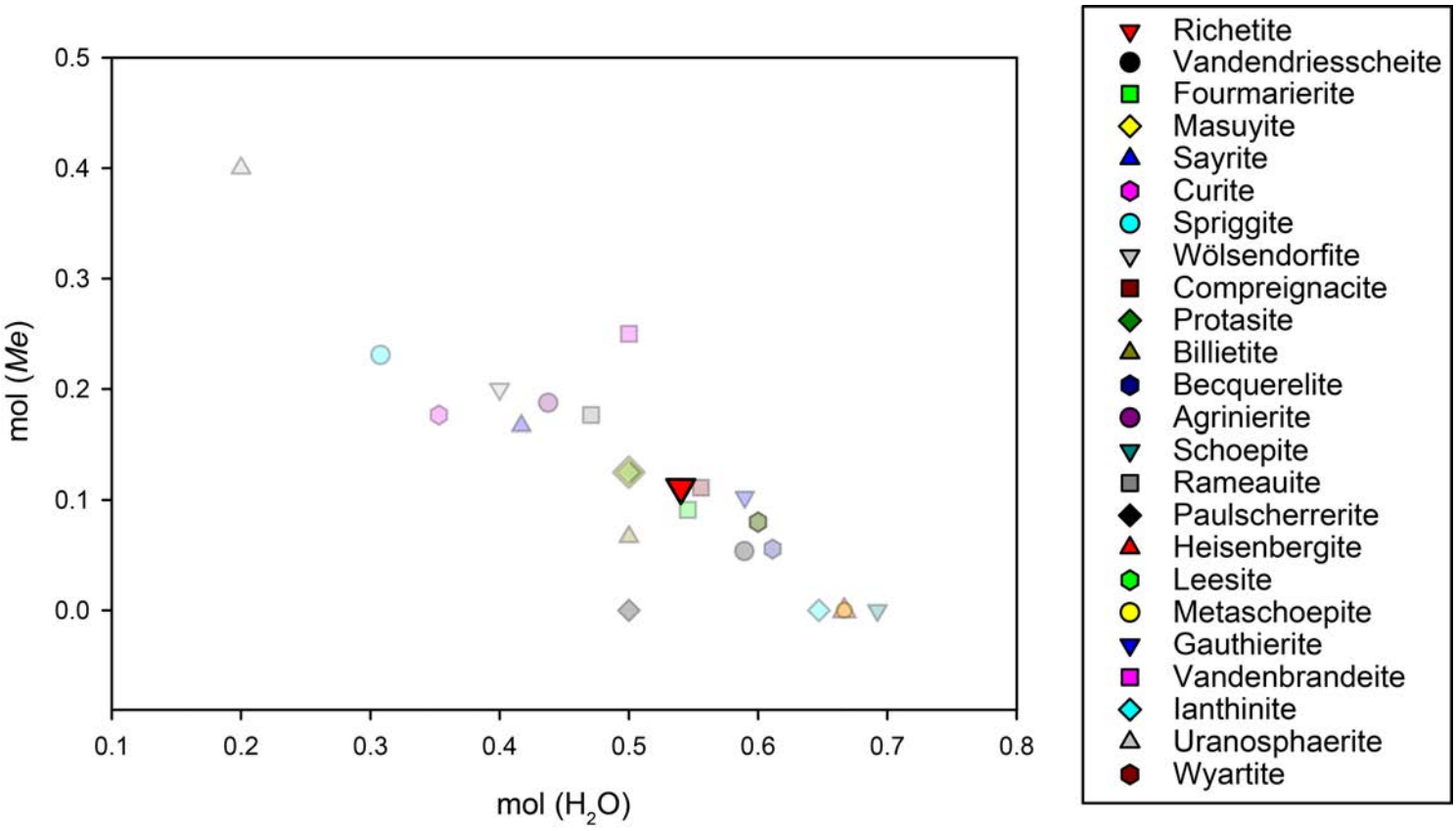

Table 1. Summary of data collection conditions and refinement parameters for richetite.

Structural formula	$(Fe^{2+}_{0.31}Mg_{0.19})Pb_{4.86}[U^{5+}(U^{6+}O_2)_{17}O_{18}(OH)_{14}](H_2O)_{\sim 19.5}$
Unit cell parameters	a = 12.0919(2), b = 16.3364(4), c = 20.2881(4) Å α = 68.800(2), β = 78.6794(18), γ = 76.1181(19)
V	3600.68(14) Å^3
Z	2
Space group	P–1
D_{calc} (g cm^{-3})	6.194 (for the formula given above)
Temperature	298 K
Diffractometer	Rigaku SuperNova, Atlas S2 CCD
Radiation (wavelength)	MoK_α (0.7107 Å)
Crystal dimensions	0.174 × 0.135 × 0.029 mm
Collection mode	ω scans to cover the Ewald sphere
Frame width, counting time	1.0°, 300 s
Limiting θ angles	3.40–28.10°
Limiting Miller indices	–15<h<15, –21<k<21, –26<l<26
No. of reflections	39599
No. of unique reflections	13469
No. of observed reflections (criterion)	9955 [I_{obs} > 3σ(I)]
μ (mm^{-1})	51.76
T_{min}/T_{max}	0.055/0.079
Coverage, R_{int}	0.98, 0.043
F_{000}	5479
Refinement	Full matrix least-squares by Jana2006 on F^2
Parameters refined	593
R, wR (obs)	0.0560, 0.1142
R, wR (all)	0.0771, 0.1210
GOF (obs, all)	1.99, 1.80
Weighting scheme	$1/(\sigma^2(I) + 0.0004I^2)$
$\Delta\sigma_{min}$, $\Delta\sigma_{max}$ (e/Å^3)	–4.12, 6.56 (1.29 Å from O70 atom)
Twin ratio; twin matrix	$0.8482(17)/0.15118(17); \begin{pmatrix} -1 & 0 & 0 \\ 0 & -0.328 & -0.671 \\ 0 & -1.328 & 0.328 \end{pmatrix}$

Table 2. Atom positions, occupation factors, displacement parameters (equivalent and isotropic, in Å^2) and bond-valence sums (in valence units) for the crystal structure of richetite.

Atom	*Occ.* (<1)	*x*/*a*	*y*/*b*	*z*/*c*	U_{eq}/U_{iso} (Å^2)	ΣBV
U1		0.56884(6)	0.32974(5)	0.40750(4)	0.0139(3)	5.93(8)
U2		1.06978(6)	0.82861(5)	−0.09742(4)	0.0137(3)	5.81(8)
U3		0.26120(6)	−0.02209(6)	0.75313(4)	0.0151(3)	6.07(8)
U4		0.42599(6)	0.16277(6)	0.57945(4)	0.0153(3)	5.95(7)
U5		0.43851(6)	0.83810(6)	−0.08721(4)	0.0160(3)	5.92(7)
U6		0.75344(6)	0.48241(5)	0.25073(4)	0.0136(3)	5.97(8)
U7		0.05207(6)	0.51722(6)	0.24384(4)	0.0150(3)	5.88(7)
U8		0.93510(6)	0.34134(6)	0.41004(4)	0.0152(3)	5.89(7)
U9		0.58292(6)	0.66312(6)	0.08266(4)	0.0160(3)	5.81(8)
U10		0.93432(6)	0.65868(6)	0.07252(4)	0.0143(3)	5.93(7)
U11		0.25508(6)	0.64896(6)	0.09384(4)	0.0165(3)	5.91(8)
U12		0.43717(7)	0.51334(6)	0.24642(4)	0.0177(3)	5.86(9)
U13		0.75112(6)	0.15270(6)	0.59592(4)	0.0158(3)	6.01(8)
U14		0.74315(6)	0.82801(5)	−0.05630(4)	0.0149(3)	5.95(8)
U15		0.54990(6)	0.02117(6)	0.74772(4)	0.0150(3)	5.91(8)
U16		0.24484(6)	0.32640(5)	0.44176(4)	0.0140(3)	5.98(8)
U17		0.08254(7)	0.16447(6)	0.57735(4)	0.0186(3)	5.37(7)
U18		−0.06322(7)	0.01441(6)	0.74493(4)	0.0197(3)	5.93(9)
Pb1	0.945(3)	0.83195(8)	−0.12157(7)	0.62331(5)	0.0317(4)	1.739(18)
Pb2	0.857(3)	0.54386(8)	0.71947(7)	0.26790(5)	0.0260(4)	1.90(2)
Pb3	0.862(3)	0.47019(9)	0.22291(8)	0.27319(5)	0.0331(5)	1.829(19)
Pb4	0.865(3)	0.18826(9)	0.36382(8)	0.63576(6)	0.0400(5)	1.772(19)
Pb5	0.776(3)	0.97785(9)	0.41404(8)	0.11436(6)	0.0260(5)	1.82(2)
Fe1/Mg1	0.62(2)/0.38(2)	1	1	0	0.018(2)	2.24(3)
Pb6	0.242(3)	0.1971(4)	0.4301(3)	0.0430(2)	0.047(2)	1.93(2)
Pb7	0.146(3)	0.03-99(5)	0.2196(4)	0.7709(3)	0.030(3)	1.89(2)
Pb8	0.142(3)	0.3150(5)	0.1421(4)	0.8660(3)	0.030(3)	1.89(2)
O1		0.0913(11)	−0.0665(9)	0.7974(7)	0.023(3)*	2.08(3)
O2		0.0981(10)	0.4323(9)	0.3675(6)	0.018(3)*	1.206(16)
O3		0.4133(13)	−0.0543(12)	0.8074(9)	0.042(5)*	2.18(4)
O4		0.4194(12)	0.2765(10)	0.4770(8)	0.027(4)*	2.12(3)
O5		0.9215(11)	0.7776(10)	−0.0263(8)	0.025(4)*	2.12(3)
O6		1.2686(10)	0.8320(8)	−0.1317(6)	0.014(3)*	1.283(19)
O7		0.5713(10)	0.2598(9)	0.3542 (6)	0.018(3)*	1.80(5)
O8		0.9032(12)	0.4544(10)	0.3083 (8)	0.026(4)*	2.09(3)
O9		0.3690(10)	0.4284(8)	0.3672 (6)	0.016(3)*	1.261(16)
O10		0.6419(11)	0.2013(9)	0.4986(7)	0.020(3)*	1.261(19)
O11		0.7685(10)	0.3286(9)	0.3719(6)	0.019(3)*	1.27(2)
O12		0.6265(11)	0.5420(9)	0.1730(7)	0.025(3)*	1.86(3)
O13		0.5863(11)	0.4432(9)	0.3063(7)	0.023(3)*	2.11(3)
O14		0.0834(12)	0.6081(10)	0.1337(7)	0.027(4)*	2.13(3)
O15		0.2550(11)	0.1902(9)	0.5404(7)	0.020(3)*	1.98(3)
O16		0.7605(11)	0.6852(9)	0.0397(7)	0.023(3)*	1.92(3)
O17		0.8854(11)	0.2093(9)	0.4979(7)	0.025(3)*	1.243(18)

O18	0.7116(12)	0.2575(10)	0.6124(7)	0.031(4)*	1.65(6)
O19	0.5745(11)	0.1264(10)	0.6393(7)	0.023(3)*	2.08(3)
O20	1.0637(11)	0.9043(9)	−0.0475(7)	0.022(3)*	1.73(6)
O21	0.3867(11)	0.7066(9)	−0.0031(7)	0.024(3)*	1.275(19)
O22	0.8698(10)	0.9315(9)	−0.1340(6)	0.019(3)*	1.219(16)
O23	0.5446(12)	1.0730(10)	−0.0756(8)	0.035(4)*	0.0158(5)
O24	0.5206(11)	0.7666(9)	−0.1382(7)	0.022(3)*	1.74(4)
O25	0.2096(10)	0.3929(9)	0.4993(6)	0.017(3)*	1.87(5)
O26	0.2083(12)	0.7539(10)	0.1094(7)	0.032(4)*	1.63(5)
O27	0.8848(11)	0.7363(9)	0.1224(7)	0.026(3)*	1.60(5)
O28	1.0774(11)	0.7525(9)	−0.1464(7)	0.023(3)*	1.67(5)
O29	1.1420(11)	0.6983(9)	−0.0045(7)	0.019(3)*	1.227(18)
O30	0.5726(11)	0.7295(9)	0.1433(7)	0.022(3)*	1.74(5)
O31	−0.0129(11)	0.6115(9)	0.2723(7)	0.024(3)*	1.93(5)
O32	0.5986(10)	0.9344(9)	−0.1298(6)	0.017(3)*	1.211(16)
O33	1.0159(11)	0.2690(9)	0.3601(7)	0.023(3)*	1.81(5)
O34	0.0688(12)	0.2863(10)	0.4863(7)	0.029(4)*	2.06(3)
O35	0.4782(11)	0.0771(9)	0.5359(7)	0.023(3)*	1.49(5)
O36	0.7707(11)	0.7686(9)	−0.1192(7)	0.023(3)*	1.63(5)
O37	0.1637(13)	0.6894(11)	0.3020(8)	0.044(4)*	0.0204(6)
O38	0.3895(11)	0.0552(9)	0.6809(7)	0.023(3)*	1.92(3)
O39	0.8560(11)	0.4142(10)	0.4595(7)	0.027(3)*	1.59(5)
O40	0.8945(11)	0.5407(9)	0.1709(7)	0.025(3)*	1.91(3)
O41	0.1386(12)	0.0414(10)	0.6659(8)	0.035(4)*	1.57(3)
O42	0.7904(11)	0.0467(9)	0.5790(7)	0.024(3)*	1.86(5)
O43	0.2763(11)	0.2681(9)	0.3779(7)	0.023(3)*	1.82(5)
O44	0.3383(9)	0.3771(8)	0.1210(6)	0.009(3)*	0.110(3)
O45	0.8009(11)	0.3875(10)	0.2179(7)	0.027(3)*	1.68(5)
O46	0.5375(12)	0.4237(10)	0.0715(7)	0.029(4)*	0
O47	0.7347(10)	0.0708(9)	0.7308(6)	0.019(3)*	1.259(18)
O48	0.2334(11)	0.5642(9)	0.2324(7)	0.023(3)*	1.237(18)
O49	0.4195(12)	0.6214(11)	0.1394(8)	0.032(4)*	2.07(3)
O50	0.4822(11)	0.1089(9)	0.7840(7)	0.022(3)*	1.93(5)
O51	0.3543(12)	0.9081(10)	−0.0377(7)	0.027(3)*	1.63(5)
O52	0.9824(11)	0.5753(9)	0.0243(7)	0.020(3)*	1.84(4)
O53	0.5674(10)	0.3984(9)	0.4601(6)	0.017(3)*	1.62(5)
O54	0.3051(11)	0.5431(9)	0.0778(7)	0.022(3)*	1.61(5)
O55	0.6269(13)	−0.0711(11)	0.7168(8)	0.040(4)*	1.80(5)
O56	0.3661(11)	0.2460(9)	0.6258(7)	0.025(3)*	1.85(5)
O57	0.3234(11)	−0.1116(10)	0.7142(7)	0.027(3)*	1.66(5)
O58	0.7074(11)	0.5843(10)	0.2783(7)	0.026(3)*	1.83(5)
O59	0.6034(12)	0.5921(10)	0.0254(7)	0.029(4)*	1.49(5)
O60	0.1217(12)	0.4186(10)	0.2184(7)	0.032(4)*	1.63(5)
O61	0.1581(12)	−0.1940(10)	0.6882(7)	0.029(4)*	0
O62	0.1175(12)	0.0890(10)	0.5142(8)	0.036(4)*	1.33(4)
O63	0.5676(10)	0.7897(9)	−0.0118(7)	0.018(3)*	2.03(4)
O64	−0.0776(12)	−0.0694(10)	0.7115(7)	0.035(4)*	1.87(6)
O65	0.4315(13)	0.4201(11)	0.2199(8)	0.038(4)*	1.69(6)
O66	−0.0643(11)	0.0997(9)	0.7798(7)	0.024(3)*	1.75(6)
O67	0.7132(10)	0.8952(9)	0.0000(6)	0.017(3)*	1.70(5)

O68		0.2040(12)	0.0675(10)	0.7909(8)	0.035(4)*	1.61(5)
O69		0.3070(14)	−0.0599(12)	0.5604(9)	0.048(5)*	0
O70		0.4776(18)	−0.0868(15)	0.6098(11)	0.081(7)*	0.210(7)
O71		1.0388(11)	−0.0868(10)	0.5766(7)	0.025(3)*	0.249(6)
O72		0.0718(15)	0.2366(13)	0.6408(9)	0.058(5)*	1.30(4)
O73		0.4279(11)	0.6030(10)	0.2808(7)	0.029(3)*	1.85(6)
O74		0.0351(14)	0.5711(12)	0.4209(9)	0.051(5)*	0.116(3)
O75		0.6599(12)	0.1895(10)	0.8039(8)	0.034(4)*	0.123(3)
O76		0.2442(11)	0.2423(10)	0.7573(7)	0.031(4)*	0.516(8)
O77		0.1987(12)	0.5527(10)	−0.0634(8)	0.035(4)*	0.415(9)
O78		1.1511(12)	0.9506(10)	0.0539(7)	0.032(4)*	0.184(6)
O79		−0.0779(13)	0.1232(11)	0.6358(8)	0.035(4)*	2.05(3)
O80		1.3589(11)	0.6965(9)	−0.1864(7)	0.024(3)*	0.191(5)
O81		0.2462(13)	0.2491(11)	0.2473(8)	0.048(5)*	0.322(6)
O82		0.9164(12)	0.9135(10)	0.0806(7)	0.029(4)*	0.297(9)
O83		0.4094(13)	0.4197(11)	0.5856(8)	0.043(4)*	0.214(4)
O84		0.3286(15)	0.5479(12)	0.4356(9)	0.056(5)*	0
O85	0.5	1.030(2)	0.278(2)	0.2254(15)	0.032(8)*	0.221(13)

*Refined with isotropic atomic displacement parameters.

This is a preprint, the final version is subject to change, of the American Mineralogist (MSA)
Cite as Authors (Year) Title. American Mineralogist, in press.
(DOI will not work until issue is live.) DOI: http://dx.doi.org/10.2138/am-2017-6092

Table 3. Interatomic distances among U atoms (in Å) in the structure of richetite.

U1–O4	2.216(12)	U2–O1^{i}	2.215(12)	U3–O1	2.256(13)
U1–O7	1.829(16)	U2–O5	2.189(12)	U3–O3	2.185(15)
U1–O9	2.657(11)	U2–O6	2.381(12)	U3–O6^{ii}	2.666(10)
U1–O10	2.355(11)	U2–O20	1.843(17)	U3–O38	2.208(12)
U1–O11	2.372(12)	U2–O22	2.658(11)	U3–O41	2.314(14)
U1–O13	2.227(12)	U2–O28	1.830(17)	U3–O57	1.849(17)
U1–O53	1.801(16)	U2–O29	2.388(11)	U3–O68	1.816(18)
<*U1–O$_{Ur}$*>	1.82	<*U2–O$_{Ur}$*>	1.84	<*U3–O$_{Ur}$*>	1.83
<*U1–O$_{eq}$*>	2.37	<*U2–O$_{eq}$*>	2.37	<*U3–O$_{eq}$*>	2.33
U4–O4	2.226(13)	U5–O3^{iii}	2.246(14)	U6–O8	2.210(15)
U4–O10	2.876(12)	U5–O6^{iv}	2.431(14)	U6–O11	2.807(11)
U4–O15	2.246(13)	U5–O21	2.342(12)	U6–O12	2.212(13)
U4–O19	2.211(14)	U5–O24	1.827(15)	U6–O13	2.233(12)
U4–O35	1.842(16)	U5–O32	2.610(14)	U6–O40	2.236(12)
U4–O38	2.217(12)	U5–O51	1.795(15)	U6–O45	1.837(17)
U4–O56	1.854(16)	U5–O63	2.211(14)	U6–O58	1.866(17)
<*U4–O$_{Ur}$*>	1.85	<*U5–O$_{Ur}$*>	1.81	<*U6–O$_{Ur}$*>	1.85
<*U4–O$_{eq}$*>	2.36	<*U5–O$_{eq}$*>	2.37	<*U6–O$_{eq}$*>	2.34
U7–O2	2.487(11)	U8–O2^{v}	2.577(14)	U9–O12	2.194(11)
U7–O8^{iv}	2.240(13)	U8–O8	2.241(13)	U9–O16	2.210(12)
U7–O14	2.208(12)	U8–O11	2.378(14)	U9–O21	3.011(14)
U7–O31	1.791(15)	U8–O17	2.371(12)	U9–O30	1.882(17)
U7–O40^{iv}	2.518(14)	U8–O33	1.817(15)	U9–O49	2.206(12)
U7–O48	2.430(14)	U8–O34^{v}	2.259(13)	U9–O59	1.868(18)
U7–O60	1.826(16)	U8–O39	1.808(16)	U9–O63	2.252(12)
<*U7–O$_{Ur}$*>	1.81	<*U8–O$_{Ur}$*>	1.81	<*U9–O$_{Ur}$*>	1.88
<*U7–O$_{eq}$*>	2.38	<*U8–O$_{eq}$*>	2.37	<*U9–O$_{eq}$*>	2.38
U10–O5	2.234(13)	U11–O14	2.247(13)	U12–O9	2.430(10)
U10–O14^{v}	2.208(13)	U11–O21	2.335(12)	U12–O12	2.525(12)
U10–O16	2.231(13)	U11–O26	1.795(17)	U12–O13	2.211(12)
U10–O27	1.821(16)	U11–O29^{iv}	2.425 14)	U12–O48	2.447(12)
U10–O29	2.770(12)	U11–O48	2.638(12)	U12–O49	2.256(13)
U10–O40	2.285(12)	U11–O49	2.241(14)	U12–O65	1.812(19)
U10–O52	1.874(16)	U11–O54	1.815(15)	U12–O73	1.810(18)
<*U10–O$_{Ur}$*>	1.85	<*U11–O$_{Ur}$*>	1.81	<*U12–O$_{Ur}$*>	1.81
<*U10–O$_{eq}$*>	2.35	<*U11–O$_{eq}$*>	2.38	<*U12–O$_{eq}$*>	2.37
U13–O10	2.378(14)	U14–O5	2.241(12)	U15–O3	2.197(13)
U13–O17	2.357(12)	U14–O16	2.433(12)	U15–O19	2.265(12)
U13–O18	1.789(17)	U14–O22	2.463(12)	U15–O32^{vi}	2.483(11)
U13–O19	2.221(12)	U14–O32	2.444(11)	U15–O38	2.419(14)
U13–O42	1.820(16)	U14–O36	1.804(17)	U15–O47	2.480(14)
U13–O47	2.566(11)	U14–O63	2.274(12)	U15–O50	1.796(15)
U13–O79v	2.247(14)	U14–O67	1.787(15)	U15–O55	1.819(16)
<*U13–O$_{Ur}$*>	1.80	<*U14–O$_{Ur}$*>	1.80	<*U15–O$_{Ur}$*>	1.81
<*U13–O$_{eq}$*>	2.35	<*U13–O$_{eq}$*>	2.37	<*U15–O$_{eq}$*>	2.37
U16–O2	2.471(11)	U17–O15	2.161(12)	U18—O1	2.222(12)
U16–O4	2.227(13)	U17–O17^{iv}	2.943(14)	U18—O22ii	2.422(10)
U16–O9	2.409(12)	U17–O34	2.166(12)	U18—O41	2.684(12)

U16–O15	2.390(12)	U17–O41	2.228(13)	U18—O47iv	2.427(12)
U16–O25	1.794(15)	U17–O62	2.005(19)	U18—O64	1.784(18)
U16–O34	2.294(13)	U17–O72	2.01(2)	U18—O66	1.774(17)
U16–O43	1.805(16)	U17–O79	2.186(12)	U18—O79	2.290(13)
<*U16–O$_{Ur}$*>	1.80	<*U17–O*>	2.24	<*U16–O$_{Ur}$*>	1.78
<*U16–O$_{eq}$*>	2.36			<*U16–O$_{eq}$*>	2.41

Symmetry codes: (i) *x*+1, *y*+1, *z*–1; (ii) *x*–1, *y*−1, *z*+1; (iii) *x*, *y*+1, *z*–1; (iv) *x*–1, *y*, *z*; (v) *x*+1, *y*, *z*; (vi) *x*, *y*–1, *z*+1; (vii) –*x*+2, –*y*, –*z*+1; (viii) –*x*+1, –*y*, –*z*+1; (ix) –*x*+1, –*y*+1, –*z*+1; (x) –*x*+1, –*y*+1, –*z*; (xi) –*x*+2, –*y*+1, –*z*; (xii) –*x*, –*y*+1, –*z*+1; (xiii) –*x*+2, –*y*+2, –*z*; (xiv) –*x*+1, –*y*+2, –*z*.

Table 4. Interatomic distances among Pb and M^{2+} sites (in Å) in the structure of richetite.

Pb1–O33^{vii}	2.613(12)	Pb2–O30	2.434(15)	Pb3–O7	2.531(16)
Pb1–O42	2.519(13)	Pb2–O50^{ix}	2.578(13)	Pb3–O24^{x}	2.664(15)
Pb1–O43^{viii}	2.998(16)	Pb2–O56^{ix}	2.874(17)	Pb3–O43	2.986(13)
Pb1–O55	2.954(13)	Pb2–O58	2.562(13)	Pb3–O55^{viii}	2.919(18)
Pb1–O62^{viii}	2.617(16)	Pb2–O73	2.535(17)	Pb3–O57^{viii}	2.710(12)
Pb1–O64^{v}	2.729(18)	Pb2–O75^{ix}	2.915(13)	Pb3–O65	2.952(15)
Pb1–O71	2.616(13)	Pb2–O76^{ix}	2.695(13)	Pb3–O70^{viii}	2.655(16)
Pb1–O81^{viii}	2.851(13)	Pb2–O83^{ix}	3.081(13)	Pb3–O80^{xi}	2.703(12)
<*Pb1–O*>	2.74	<*Pb2–O*>	2.71	Pb3–O81	2.766(13)
				<*Pb3–O*>	2.77
Pb4–O25	2.606(12)	Pb5–O28^{xi}	2.772(15)	Pb6–O16^{x}	2.847(17)
Pb4–O31^{xii}	2.591(12)	Pb5–O40	2.623(16)	Pb6–O36^{x}	3.013(14)
Pb4–O56	2.548(12)	Pb5–O45	2.683(12)	Pb6–O44	2.350(13)
Pb4–O58^{ix}	2.798(18)	Pb5–O52	2.613(12)	Pb6–O52^{iv}	3.051(12)
Pb4–O72	2.73(2)	Pb5–O52^{xi}	2.707(15)	Pb6–O52^{x}	2.811(16)
Pb4–O74^{xii}	2.949(14)	Pb5–O60^{v}	3.023(16)	Pb6–O54	2.839(18)
Pb4–O76	2.637(12)	Pb5–O77^{x}	2.417(14)	Pb6–O59^{x}	2.554(12)
Pb4–O83	2.905(13)	Pb5–O85	2.58(3)	Pb6–O77	2.359(14)
<*Pb4–O*>	2.72	<*Pb5–O*>	2.68	<*Pb6–O*>	2.72
Pb7–O27^{ix}	2.871(18)	Pb8–O23^{vi}	3.039(14)	M^{2+}–O20	2.046(16)
Pb7–O31^{xii}	2.534(15)	Pb8–O27^{ix}	2.768(13)	M^{2+}–O20^{xiii}	2.046(16)
Pb7–O37^{xii}	2.924(14)	Pb8–O30^{ix}	2.693(17)	M^{2+}–O78	2.148(13)
Pb7–O66	2.507(17)	Pb8–O50	2.439(13)	M^{2+}–O78^{xiii}	2.148(13)
Pb7–O68	2.744(14)	Pb8–O67^{ix}	2.533(13)	M^{2+}–O82	2.013(12)
Pb7–O72	2.511(19)	Pb8–O68	2.93(2)	M^{2+}–O82^{xiii}	2.013(12)
Pb7–O76	2.529(15)	Pb8–O76	2.394(13)	<M^{2+}–*O*>	2.07
Pb7–O82^{ix}	3.073(13)	Pb8–O82^{ix}	3.023(14)		
<*Pb7–O*>	2.71	<*Pb8–O*>	2.73		

Symmetry codes: (i) *x*+1, *y*+1, *z*–1; (ii) *x*–1, *y*−1, *z*+1; (iii) *x*, *y*+1, *z*–1; (iv) *x*–1, *y*, *z*; (v) *x*+1, *y*, *z*; (vi) *x*, *y*–1, *z*+1; (vii) –*x*+2, –*y*, –*z*+1; (viii) –*x*+1, –*y*, –*z*+1; (ix) –*x*+1, –*y*+1, –*z*+1; (x) –*x*+1, –*y*+1, –*z*; (xi) –*x*+2, –*y*+1, –*z*; (xii) –*x*, –*y*+1, –*z*+1; (xiii) –*x*+2, –*y*+2, –*z*; (xiv) –*x*+1, –*y*+2, –*z*.

Table 5. Comparison of the U17Φ_7 polyhedral geometry in richetite with other compounds.

				U–Φ (Å)				O–U–O (°)	BV (v.u.)	Ref.
Richetite (U17)	2.161	2.943	2.166	2.228	2.01	2.01	2.186	171.8	5.37	this work
Wyartite (U3)	2.07	2.09	2.06	2.14	2.44	2.47	2.480	167.0	5.07	1
Dehyd. wyartite (U2)	2.095	2.095	2.092	2.092	2.476	2.512	2.301	163.6	5.10	2
U_2MoO_8	2.06	2.06	2.11	2.18	2.36	2.46	2.73	178.1	4.92	3
	2.08	2.08	2.13	2.15	2.32	2.35	2.58	164.1	5.12	
$USbO_3$	1.93	2.02	2.13	2.30	2.35	2.43	2.50	173.0	5.23	4
UVO_5	2.05	2.07	2.21	2.21	2.30	2.30	2.32	179.9	5.26	5
$U_5O_{12}Cl$	2.06	2.06	2.25	2.25	2.30	2.30	2.54	178.9	4.95	6

1 = Burns and Finch (1999); 2 = Hawthorne et al. (2006); 3 = Serezhkin et al. (1973); 4 = Dickens and Stuttard (1992); 5 = Dickens et al. (1992); 6 = Cordfunke et al. (1985).